Loss of coherence in interferometry

S. M. Tan and D. F. Walls
Department of Physics, University of Auckland, Auckland, New Zealand
(Received 2 December 1992)

We present a unified treatment of a number of double-slit experiments which give "which-path" information. The loss of coherence is described by a random-average model over basis states of the path detector. While the precise physical mechanism depends on the choice of the detector basis, the random-average model shows that the loss of coherence may always be described in terms of a stochastic disturbance to the system due to coupling with the path detector. The possibility of quantum erasers is shown to arise naturally from an appropriate choice of detector basis.

PACS number(s): 03.65.Bz, 07.60.Ly, 42.50.Vk

I. INTRODUCTION

Young's double-slit experiment provides perhaps the simplest example in which the coherent addition of quantum-mechanical amplitudes leads to interference. When a "which-path" detector is introduced in order to monitor which slit the particle passes through, the principle of complementarity states that the interference is necessarily destroyed. The detection of path information necessarily involves an interaction which couples the particles to the detector. It is convenient to call the particles and the double slit the "system" and the path detector the "environment" to which they couple.

Elementary considerations (summarized in Sec. II) show that the degree of coherence loss depends on the inner product between the states of the environment which couple to the two possible particle paths. In particular, if the environment states are orthogonal, these paths are perfectly distinguishable and all interference is lost. From the point of view of the system, however, it is natural to view this destruction of interference predicted by the complementarity principle as a "disturbance" introduced by the coupling to the environment. Indeed Stern, Aharonov, and Imry [1] state that the effect on the system may always be regarded as a randomization of the interfering particle's phase and they rewrite the degree of coherence loss as an expectation value of the form $\langle e^{i\phi} \rangle$ where the average is taken over some probability density function $P(\phi)$ for this random phase.

Various schemes have been proposed as path detectors for the double-slit experiment, including Einstein's recoiling slit [2, 3] in which the momentum imparted to a slit placed in front of the double slit is measured and Feynman's light microscope [4] in which the detector is light scattered from electrons going through a double slit. In Feynman's discussion of the double-slit experiment, he concludes that "If an apparatus is capable of determining which hole the electron goes through, it *cannot* be so delicate that it does not disturb the pattern in an essential way. No one has ever found (or even thought of) a way around the uncertainty principle."

The involvement of the uncertainty principle and the idea of random dephasing has led to the idea that the disturbance on the system is somehow uncontrollable. Recently, a proposal has been made which is said to circumvent this limitation, which is able "to obtain which-path or particlelike information without scattering or otherwise introducing large uncontrolled phase factors into the interfering beams" [5]. As shown in Fig. 1, the interfering particles are Rydberg atoms which are initially excited by a laser beam. An empty micromaser cavity is placed in front of each slit and the interaction time is adjusted so that it is certain that the excited atom deexcites, leaving a photon in the cavity through which it passes. Calculations of the effect of a single micromaser cavity on an excited atom [6] show that there is no change in the center-of-mass momentum of the atom and only a small change in position when the atom passes through the cavity. It is concluded on the basis of this that "the question of how the principle of complementarity is enforced must then be readdressed" since "it is simply the information contained in a functioning measuring apparatus that changes the outcome of the experiment, and not uncontrolled alterations of the spatial wave function, resulting from the action of the measuring apparatus on the system under observation." As further evidence of the lack of uncontrollable scattering events, it is then shown that a quantum eraser can be devised which allows an interference pattern of high visibility to be extracted from within a featureless pattern if a suitable measurement is made on the path detector which erases the path information. This is said to be a special feature of this new configuration, since "if we considered the coherence to be lost because of a random scattering

FIG. 1. Double-slit configuration with micromaser cavities as path detectors.

or other stochastic perturbations, this question (of the possibility of a quantum eraser) would never come up."

In this paper we shall present a unified treatment of a variety of configurations designed to illustrate the complementarity principle and demonstrate their underlying similarities. We show that although the degree of coherence loss can always be calculated abstractly in terms of inner products of environment states, it is always possible to construct many random-average models for the process in which the final interference pattern is always expressed as a stochastic average of conditional patterns. The multiplicity of models arises from the different ways in which one can choose to describe the path detector or environment. If we do not measure the final state of the path detector, it is necessary to average over the conditional interference patterns and all of the alternative models yield the same result for the final pattern. This is a stochastic average insofar as the final state of the path detector can only be described probabilistically. On the other hand, if the path-detector state is measured, it is possible to correlate this information with the final position of the particle. We shall see that in certain cases, the measurement of the path detector gives a precise indication of the way in which the system wave function has been disturbed. Depending on what we choose to measure, the nature of this disturbance can sometimes be interpreted as a momentum kick or as a localization of the particle. In the former case, the conditional interference pattern has unit visibility (but is shifted) whereas in the latter, the conditional interference pattern is featureless. The presence of such high visibility conditional interference patterns is the basis of the quantum eraser and we shall see how such erasers can be constructed for all the configurations analyzed. We emphasize that loss of coherence can always be described in terms of an alteration of the system state due to the coupling with the detector. Although this involves a stochastic average over the detector states, it does not imply that the alteration of the system is "uncontrolled" unless information about the detector state is discarded.

In Sec. II, we present the general analysis of two-slit systems coupled to path detectors and in Sec. III introduce probabilistic average models for explaining the loss of coherence. In Secs. IV and V, the analysis is applied to the Einstein recoiling slit and a variant of the Feynman light microscope (using atoms rather than electrons). In Sec. VI, we analyze the configuration of Fig. 1 with micromaser cavities, showing the similarities to the previous configurations and also apply the technique to a different problem, the calculation of the loss of coherence when these cavities are initially filled with coherent microwave radiation.

II. YOUNG'S INTERFERENCE WITH WHICH-PATH DETECTORS

Consider a Young's interference experiment for atoms of mass m together with a which-path detector (see Fig. 2). For definiteness, we suppose that the atoms are propagating along the z direction with a well-defined longitudinal momentum $p_z = \hbar k$ which is large compared to the transverse momentum changes during the course of the experiment. This allows us to work in the paraxial approximation throughout. We shall ignore the y coordinate in the analysis. The screen with the double slit is taken to be in the plane $z = 0$ with the narrow slits spaced d apart at positions $x = \xi_1 = \frac{1}{2}d$ and $x = \xi_2 = -\frac{1}{2}d$. Starting with a plane atomic wave and assuming infinitesimally wide slits, the state immediately after passing through the double slit (at time t_1) is a coherent superposition of position eigenstates

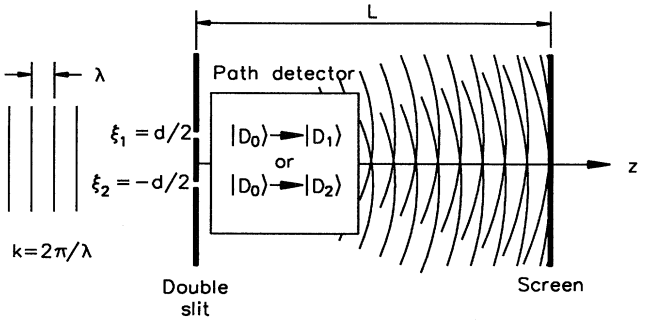

FIG. 2. General double-slit configuration with path detectors.

$$|\psi(t_1^+)\rangle = \frac{1}{\sqrt{2}}\left(|\xi_1\rangle + |\xi_2\rangle\right). \tag{1}$$

If we first suppose that no path detector is present, the atom propagates freely to the screen (located in the plane $z = L$) under the unitary time evolution $U(t_2, t_1)$ for free motion with the Hamiltonian

$$H = \frac{p^2}{2m}. \tag{2}$$

Thus when the atom hits the screen,

$$|\psi(t_2)\rangle = \frac{1}{\sqrt{2}}U(t_2, t_1)\left(|\xi_1\rangle + |\xi_2\rangle\right) \tag{3}$$

$$= \frac{1}{\sqrt{2}}\int_{-\infty}^{\infty}[\psi_1(x) + \psi_2(x)]|x\rangle\, dx, \tag{4}$$

where

$$\psi_\ell(x) = \langle x\,|U(t_2, t_1)|\,\xi_\ell\rangle \propto \exp\left(i\frac{m(x-\xi_\ell)^2}{2\hbar(t_2 - t_1)}\right) \tag{5}$$

is the probability amplitude for detecting the atom at x on the screen given that the atom passed through slit ℓ. We shall not be concerned with the normalization constant in this discussion.

Under the assumption that the longitudinal momentum remains approximately constant at p_z throughout the interaction, the time of passage between double slit and screen is mL/p_z. We can then write

$$\psi_\ell(x) \propto \exp\left(\frac{ik(x-\xi_\ell)^2}{2L}\right). \tag{6}$$

From Eq. (4), the probability density for detecting an atom at position x on the screen is

$$|\langle x|\psi(t_2)\rangle|^2 = \tfrac{1}{2}\,[|\psi_1(x)|^2 + |\psi_2(x)|^2 + 2\,\mathrm{Re}\{\psi_1^*(x)\psi_2(x)\}]. \tag{7}$$

Substituting the expressions for ψ_1 and ψ_2 in the situation of infinitesimally wide slits,

$$|\langle x|\psi(t_2)\rangle|^2 \propto 1 + \cos\left(\frac{kdx}{L}\right), \tag{8}$$

which is the familiar two-slit interference pattern with unit visibility.

We now include the effect of the path detector. We shall treat the path detector also as a quantum-mechanical system which is initially in a pure state $|D_0\rangle$. As a result of the interaction between the atom and the path detector, by the time the atom hits the screen, the detector has evolved either into state $|D_1\rangle$ or into state $|D_2\rangle$ depending on the path taken by the atom. The joint state of the system and the path detector at time t_2 is thus given by

$$|\psi(t_2)\rangle = \frac{1}{\sqrt{2}}\int_{-\infty}^{\infty}[\psi_1(x)|D_1\rangle + \psi_2(x)|D_2\rangle]|x\rangle\,dx. \tag{9}$$

This is an entangled state of the system and the path detector. If we again ask for the probability density that the atom be found at position x on the screen, we need to compute

$$|\langle x|\psi(t_2)\rangle|^2 = \mathrm{tr}\,[|\psi(t_2)\rangle\langle\psi(t_2)|\,|x\rangle\langle x|] \tag{10}$$

$$= \tfrac{1}{2}[|\psi_1(x)|^2 + |\psi_2(x)|^2 + 2\,\mathrm{Re}\{\psi_1^*(x)\psi_2(x)\langle D_1|D_2\rangle\}]. \tag{11}$$

The interference term has the additional factor $\langle D_1|D_2\rangle$ which causes the visibility to be reduced by $|\langle D_1|D_2\rangle|$. If the detector states $|D_1\rangle$ and $|D_2\rangle$ are orthogonal, it becomes possible to distinguish them with certainty and the interference disappears. On the other hand, if the detection process is less efficient, the overlap between $|D_1\rangle$ and $|D_2\rangle$ is larger and partial interference remains.

Note that the states $|D_1\rangle$ and $|D_2\rangle$ depend only on the initial state $|D_0\rangle$ and the nature of the interaction and not on the way in which we subsequently choose to observe the path detector. If we do not consider the result of observing the path detector, the inner product $\langle D_1|D_2\rangle$ completely characterizes the degree of coherence loss as a result of the coupling to the path detector.

III. THE RANDOM-AVERAGE MODEL FOR COHERENCE LOSS

We now consider how the loss of coherence predicted by (9) can be explained in terms of a random-average model. In this model, the final interference pattern is viewed as a sum of non-negative partial interference patterns just as a marginal probability density is obtained by summing over variables in a joint probability density. The joint probability which we shall consider is one which involves the state of the path detector and the position of the atom on the screen. Although $|D_1\rangle$ and $|D_2\rangle$ are the detector states which couple to the atomic paths, we are free to measure any observable property of the detector. The eigenstates of the chosen observable form the pointer basis of the measurement which we shall denote by $|B_\beta\rangle$. Without loss of generality we may assume the pointer basis to be orthonormal. The joint probability density for observing the path detector in state $|B_\beta\rangle$ and the atom at position x is given by

$$P(B_\beta, x) = \mathrm{tr}\,[|\psi(t_2)\rangle\langle\psi(t_2)|\,|B_\beta\rangle\langle B_\beta|\,|x\rangle\langle x|] \tag{12}$$

$$= \tfrac{1}{2}|\langle B_\beta|D_1\rangle\psi_1(x) + \langle B_\beta|D_2\rangle\psi_2(x)|^2 \tag{13}$$

$$= \tfrac{1}{2}[|\psi_1(x)\langle B_\beta|D_1\rangle|^2 + |\psi_2(x)\langle B_\beta|D_2\rangle|^2 + 2\,\mathrm{Re}\{\psi_1^*(x)\langle D_1|B_\beta\rangle\psi_2(x)\langle B_\beta|D_2\rangle\}]. \tag{14}$$

Summing these partial interference patterns over all possible states of the detector $|B_\beta\rangle$ yields the total interference pattern

$$P(x) = \int P(B_\beta, x)\,d\beta = \tfrac{1}{2}[|\psi_1(x)|^2 + |\psi_2(x)|^2 + 2\,\mathrm{Re}\{\psi_1^*(x)\psi_2(x)\langle D_1|D_2\rangle\}], \tag{15}$$

where we have used the completeness and orthonormality of the detector states. As expected, this result is the same as (9) when the detector is present but its final state is ignored.

We may similarly ask for the probability that the detector be found in state $|B_\beta\rangle$ when we ignore the final position of the atom. Since the interference term has zero mean,

$$P(B_\beta) = \int P(x, B_\beta)\,dx = \tfrac{1}{2}[|\langle B_\beta|D_1\rangle|^2 + |\langle B_\beta|D_2\rangle|^2]. \tag{16}$$

Figure 3 shows a schematic representation of the forma-

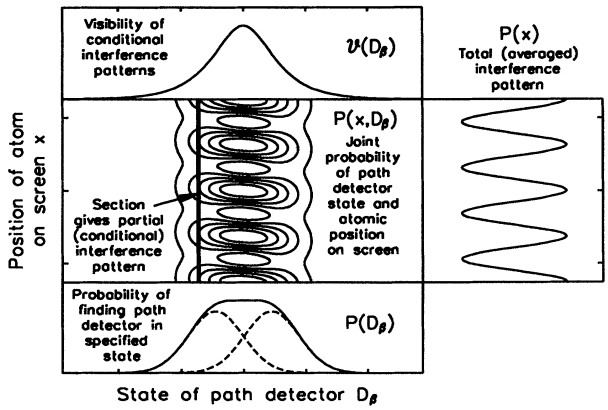

FIG. 3. Schematic representation of joint and marginal probability distributions in the random average model for the double-slit configuration with path detectors. The dashed lines below the marginal probability distribution for the path detector (which sum to give the solid line) show the joint probability that the atom went through a particular slit leaving the path detector in the specified state.

tion of these marginal distributions from the joint distribution in the random-average model of coherence loss. This graphical format will be used to present many of the subsequent results in this paper. The joint distribution is represented as a contour plot of $P(B_\beta, x)$. To its right is a plot of the total interference pattern $P(x)$. Below the joint distribution is a plot of the probability density of finding the detector in state $|B_\beta\rangle$, namely, $P(B_\beta)$. According to (16), this is a sum of $\frac{1}{2}|\langle B_\beta|D_1\rangle|^2$ and $\frac{1}{2}|\langle B_\beta|D_2\rangle|^2$ and so these are plotted as dashed lines below $P(B_\beta)$. The ratio of these quantities is the relative probability that the atom passed through each slit given that the detector is found in state $|B_\beta\rangle$. Each vertical section through the joint probability distribution is a partial interference pattern which is associated with a particular measurement of the detector. The visibility of such partial interference patterns indicates to what extent the measurement of the path detector has localized the atom and is given by

$$\mathcal{V}(B_\beta) = \frac{2|\langle B_\beta|D_1\rangle||\langle B_\beta|D_2\rangle|}{|\langle B_\beta|D_1\rangle|^2 + |\langle B_\beta|D_2\rangle|^2}. \tag{17}$$

This will be called the conditional visibility function and it is plotted above the joint distribution.

As an alternative to regarding the total interference pattern as a sum of partial interference patterns, we may consider it as a weighted average of conditional interference patterns

$$P(x) = \int P(x|B_\beta)P(B_\beta)\,d\beta \tag{18}$$

and $P(x|B_\beta)$ is the conditional interference pattern given that the detector is found in state $|B_\beta\rangle$

$$P(x|B_\beta) = P(x, B_\beta)/P(B_\beta). \tag{19}$$

The conditional interference patterns are simply normalized versions of the partial interference patterns.

The form of the partial interference patterns given by (13) suggests an interpretation in terms of the effect of measuring the path detector on the double-slit system. We see that if we measure the detector to be in state $|B_\beta\rangle$, the effect on the interference pattern is as if the complex amplitudes at the slits were changed to partial amplitudes $\langle B_\beta|D_1\rangle$ and $\langle B_\beta|D_2\rangle$. The partial interference patterns may be thought of as having been produced by these partial amplitudes. Since there are many possible alternative sets of pointer bases for the path detector, we can construct different sets partial interference patterns and different physical models for the dynamical effect of the measurement of the path detector. However, once we sum over all possible results of measurement, we recover the same total interference pattern (9). These considerations will now be illustrated for several specific examples.

IV. THE EINSTEIN RECOILING SLIT

Following Wooters and Zurek [7], we consider the configuration shown in Fig. 4 in which a movable screen with a single slit in it is placed in the plane $z = -L$ in front of the double slit in the plane $z = 0$. The two slits are fixed at $x = \xi_1 = \frac{1}{2}d$ and $x = \xi_2 = -\frac{1}{2}d$. The interference pattern is detected on the screen in the plane $z = L$. The screen with the single slit acts as the path detector. In the context of the following discussion we will again refer to the interfering particles as atoms and consider these to be incident along the z direction with a well-defined longitudinal momentum $p_z = \hbar k$ and zero transverse momentum. Of course, only a small fraction of the incident atoms get through the two screens with the slits and in this analysis we are effectively ignoring all trials in which the incident atom is absorbed by a collision with one of the first two screens.

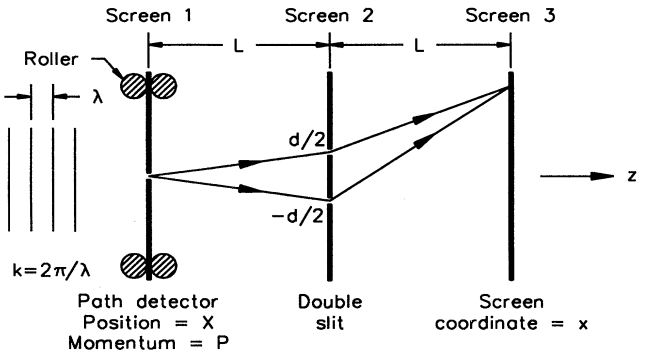

FIG. 4. The Einstein recoiling slit configuration. The first screen with a single slit acts as a path detector for the path of the atom through the double slit in the second screen. The interference pattern forms on the third screen.

At time $t = 0$, we suppose that an atom passes through the first screen with the single slit. We adopt an idealized model for the interaction of the atom and the slit by introducing an interaction potential which is zero when the atom is within the slit and infinite outside. If we denote the position eigenstates of the screen with the slit by $|X\rangle_S$ (where X denotes the position of the slit) and those of the atom by $|x_1\rangle_A$, the effect of the interaction is to cause an initial joint state $|x_1\rangle_A|X\rangle_S$ to evolve to zero if $x_1 \neq X$ and to be unchanged if $x_1 = X$. This evolution is nonunitary since we assume that atoms which miss the slit and hit the screen are of no further interest.

Corresponding to the initial path-detector state $|D_0\rangle$ in the general analysis, we need to specify an initial state for the screen with the single slit. This will be taken to be the minimum uncertainty state

$$|D_0\rangle \propto \int \exp\left(-\frac{X^2}{2\sigma^2}\right)|X\rangle_S\,dX. \tag{20}$$

We shall assume that on each trial, the first screen is reinitialized to this state. Since the initial atomic state has zero (transverse) momentum, the joint state of atom and path detector after the atom passes through the first screen is

$$|\psi(0^+)\rangle \propto \int\int \exp\left(-\frac{X^2}{2\sigma^2}\right)\delta(x_1-X)|x_1\rangle_A|X\rangle_S\,dx_1\,dX = \int \exp\left(-\frac{X^2}{2\sigma^2}\right)|X\rangle_A|X\rangle_S\,dX. \quad (21)$$

This state evolves on the way to the second screen where the atom interacts with the double slit. This selects out the portion of the wave function at the position of the slits ξ_1 and ξ_2. Further propagation to the final screen yields the joint state

$$|\psi\rangle \propto \int\int \exp\left(-\frac{X^2}{2\sigma^2}\right)\left\{\exp\left(\frac{ik(\xi_1-X)^2}{2L}\right)\psi_1(x)+\exp\left(\frac{ik(\xi_2-X)^2}{2L}\right)\psi_2(x)\right\}|x\rangle_A(U_S|X\rangle_S)\,dx\,dX, \quad (22)$$

where U_S denotes operator describing the time evolution of the first screen during the time that the atom takes to travel to the final screen. Since the mass of the screen is very large compared to the mass of the atom, this time evolution does not appreciably change the wave function of the screen in the position representation and we may approximate U_S by the identity on this timescale.

Equation (22) may be written in the form (9) if we define $|D_1\rangle$ and $|D_2\rangle$ which are the detector states coupling to each of the possible atomic paths by

$$|D_\ell\rangle \propto \int \exp\left[-\left(\frac{1}{2\sigma^2}-\frac{ik}{2L}\right)X^2 - \frac{ik\xi_\ell X}{L}+\frac{ik\xi_\ell^2}{2L}\right]|X\rangle\,dX. \quad (23)$$

The constant of proportionality can easily be found by normalization and we find that the inner product $\langle D_1|D_2\rangle$ is

$$\mathcal{V}=\langle D_1|D_2\rangle=\exp\left[-\left(\frac{k(\xi_2-\xi_1)\sigma}{2L}\right)^2\right]. \quad (24)$$

This is the visibility of the total interference pattern as a result of including the recoiling slit. We note that the visibility falls either when the slit separation increases so that the fringes are more closely spaced or when the initial position uncertainty of the path detector is increased.

Having obtained the above result by the mathematical operation of calculating the inner product of the possible final states of the single slit, we now consider two alternative ways of obtaining the same result by using the random-average model in which we take a probabilistic average of conditional interference patterns.

A. Measuring the momentum of the slit

Suppose that as our pointer basis for the detector (i.e., the single slit) we choose the momentum eigenstates $|P\rangle$. It is easy to verify that

$$\langle P|D_\ell\rangle \propto \exp\left[-\frac{\sigma^2L\,(P/\hbar+k\xi_\ell/L)^2}{2(L-ik\sigma^2)}+\frac{ik\xi_\ell^2}{2L}\right]. \quad (25)$$

Given that the measured slit momentum is P, $|\langle P|D_\ell\rangle|^2/(|\langle P|D_1\rangle|^2+|\langle P|D_2\rangle|^2)$ is the probability that the atom went through slit ℓ. Since this depends on the value of the measurement P, it gives some information about the path taken.

From these inner products we find the joint probability density

$$P(P,x)\propto|\langle P|D_1\rangle|^2+|\langle P|D_2\rangle|^2 + 2\,\mathrm{Re}[\langle P|D_1\rangle^*\langle P|D_2\rangle\exp(ikdx/L)]. \quad (26)$$

Integrating over x to find the probability that the slit momentum is P yields

$$P(P)\propto\exp\left[-\frac{(P+\overline{P})^2}{2(\Delta P)^2}\right]+\exp\left[-\frac{(P-\overline{P})^2}{2(\Delta P)^2}\right], \quad (27)$$

where $\overline{P}=\hbar kd/(2L)$ and

$$\Delta P=\hbar\sqrt{1/(2\sigma^2)+(k\sigma)^2/(2L^2)}.$$

This is the sum of two Gaussian functions centered at $\pm\overline{P}$ with width ΔP. Each Gaussian function arises from the momentum transfer which deflects the atom to either one slit or the other. If these Gaussian functions are well separated, it is possible to determine the path taken by the atom. The condition that $\overline{P}\gg\Delta P$ is equivalent to

$$\left(\frac{L}{kd\sigma}\right)^2+\left(\frac{\sigma}{d}\right)^2\ll\sqrt{2} \quad (28)$$

and so we see that if the peaks are well separated, it follows that $kd\sigma/L$ must be large and so the visibility given by (24) is necessarily small. However, the converse is *not* true and it is possible to have a low visibility even though the screen momentum gives no path information.

Integrating over P on the other hand yields a total interference pattern

$$P(x)\propto 1+\exp\left(-\left[\frac{kd\sigma}{2L}\right]^2\right)\cos\left(\frac{kdx}{L}\right) \quad (29)$$

which has the visibility predicted by (24).

We may now consider the conditional interference pattern given that the slit momentum has been measured to be P. The visibility of the conditional interference pattern is

$$\mathcal{V}(P)=\frac{2|\langle P|D_1\rangle||\langle P|D_2\rangle|}{|\langle P|D_1\rangle|^2+|\langle P|D_2\rangle|^2}=\frac{1}{\cosh[P\overline{P}/(\Delta P)^2]}. \quad (30)$$

This is always unity when $P = 0$ and falls for larger P. Depending on the relative probabilities of various values of P, the conditional interference patterns contribute with different weights to the total interference pattern.

The phase shift of the conditional pattern (which determines the location of the central fringe) is

$$\Phi(P) = \arg(\langle P|D_1\rangle^*\langle P|D_2\rangle) = \frac{k\sigma^2}{L}\left(\frac{P\overline{P}}{(\Delta P)^2}\right). \quad (31)$$

In Figs. 5(a) through 5(c) we show how these results appear in graphical form. The axes are labelled with dimensionless versions of the detector momentum $Pd/\hbar$ and atomic position kdx/L. The parameters for Fig. 5(a) are $d/L = 10^{-4}$, $kd = 16\times10^4$, $\sigma/d = \frac{1}{4}$. We see that the two Gaussian functions which make up $P(P)$ are quite well separated so that the path is well determined by the measurement. As expected, the visibility is small (≈ 0.018). The graph of $\mathcal{V}(P)$ clearly shows that in for

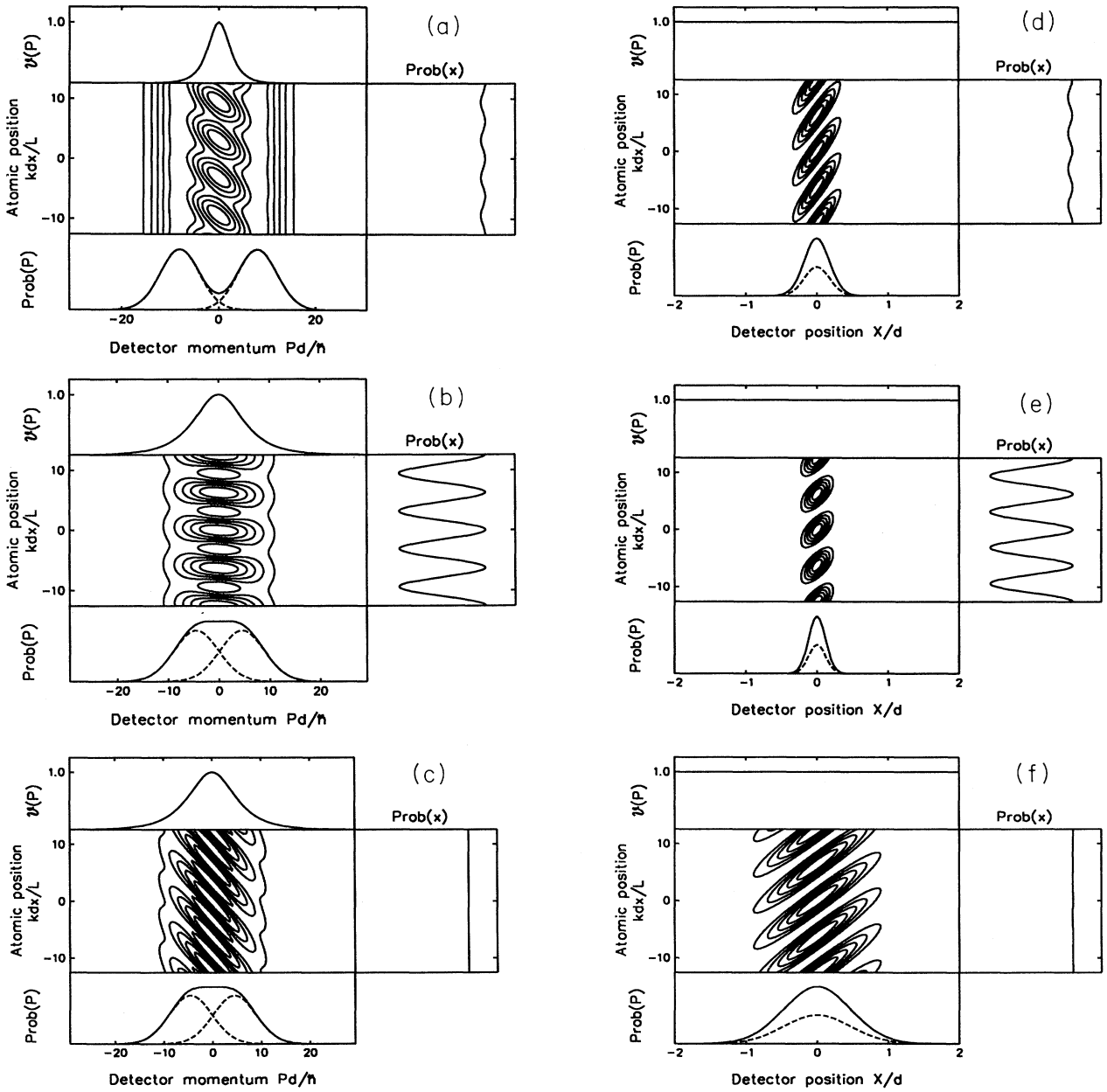

FIG. 5. Random-average model plots for the Einstein recoiling slit. Plots (a), (b), and (c) are for a measurement of the momentum of the first screen while (d), (e), and (f) are for a meaurement of the position of the first screen. Parameter values for (a) and (d) are $d/L = 10^{-4}$, $kd = 16\times10^4$, $\sigma/d = \frac{1}{4}$ and the resulting visibility is about 0.018. Parameter values for (b) and (e) are $d/L = 10^{-4}$, $kd = 9\times10^4$, $\sigma/d = \frac{1}{6}$ and the resulting visibility is about 0.56. Parameter values for (c) and (f) are $d/L = 10^{-4}$, $kd = 9\times10^4$, $\sigma/d = \frac{2}{3}$ and the resulting visibility is about 1.23×10^{-4}. Refer to Fig. 3 for the key to these plots.

the probable final values of the screen momentum P, the conditional visibility is small and so the final interference pattern is largely the average of low-visibility patterns. Physically, we would express this by saying that the measurement of the screen momentum often leads to a good localization of the atom to one or other slit. Since the single-slit patterns are featureless, the average of these is also featureless.

In Fig. 5(b), the parameters are altered to $d/L = 10^{-4}$, $kd = 9 \times 10^4$, $\sigma/d = \frac{1}{6}$. For these values, the Gaussian functions making up $P(P)$ overlap considerably and so which-path information is not available. The conditional visibility $\mathcal{V}(P)$ is high for the range of probable final screen momenta and the average of the conditional interference patterns results in an overall pattern of high visibility (≈ 0.56).

In Fig. 5(c), the parameters are $d/L = 10^{-4}$, $kd = 9 \times 10^4$, $\sigma/d = \frac{2}{3}$. Although the graphs for $P(P)$ and $\mathcal{V}(P)$ are identical with those of Fig. 5(b) so that which-path information cannot be deduced from the measurement and the conditional visibility is high for the probable values of P, the overall visibility is very small ($\approx 1.23 \times 10^{-4}$). The reason for this is clear from the contours of the joint probability which show that the patterns which are being averaged together do not line up, but are shifted relative to each other so that the fringes are washed out. The difference between Figs. 5(b) and 5(c) thus arises from the behavior of the function $\Phi(P)$. This example shows that not having path information is a necessary but insufficient condition for an interference pattern of high visibility.

B. Measuring the final position of the slit

We now suppose that we measure the final position of the detector, effectively choosing the position eigenstates as the pointer basis $|X\rangle$ for the single slit. Although these are not stationary states of the detector Hamiltonian, the large mass of the detector means that the amount of spreading of the wave function over the transit time of the atom can be made insignificant.

In this case,

$$\langle X|D_\ell\rangle \propto \exp\left[-\left(\frac{1}{2\sigma^2}-\frac{ik}{2L}\right)X^2-\frac{ik\xi_\ell}{L}X+\frac{ik\xi_\ell^2}{2L}\right]. \tag{32}$$

Since $|\langle X|D_1\rangle| = |\langle X|D_2\rangle|$ for all X, the conditional probability that the atom passes through slit ℓ given a measurement of the single-slit position is always $\frac{1}{2}$. Measurement of the position of the single slit thus gives no information about the path taken for any values of the parameters.

The joint probability density for atom and slit is

$$P(X,x) \propto |\langle X|D_1\rangle|^2 + |\langle X|D_2\rangle|^2 + 2\,\mathrm{Re}[\langle X|D_1\rangle^*\langle X|D_2\rangle \exp(ikdx/L)] \tag{33}$$

$$= 2\exp(-X^2/\sigma^2)[1+\cos\{kd(x+X)/L\}]. \tag{34}$$

Integrating over x to find the probability that the slit position is X yields

$$P(X) \propto \exp(-X^2/\sigma^2). \tag{35}$$

Similarly, integrating over X to find the total interference pattern yields

$$P(x) \propto 1+\exp\left(-\left[\frac{kd\sigma}{2L}\right]^2\right)\cos\left(\frac{kdx}{L}\right) \tag{36}$$

which is identical to the result obtained earlier.

The conditional interference pattern given that the slit position has been measured to be X has visibility

$$\mathcal{V}(X) = \frac{2|\langle X|D_1\rangle||\langle X|D_2\rangle|}{|\langle X|D_1\rangle|^2+|\langle X|D_2\rangle|^2} = 1 \tag{37}$$

and the phase shift is

$$\Phi(X) = \arg(\langle X|D_1\rangle^*\langle X|D_2\rangle) = kdX/L. \tag{38}$$

Unlike the situation in which the momentum of the single slit is measured, the conditional interference patterns all have visibility equal to 1. The reduction of visibility when these patterns are averaged together results only from the different phase shifts washing out the fringes. Figures 5(d), 5(e), and 5(f) show the joint and marginal probability functions when the single-slit position is measured for the same sets of parameter values as Figs. 5(a), 5(b), and 5(c), respectively. The total interference patterns are identical for the corresponding pairs of graphs, but our physical explanations for the loss of coherence differ. For example, in Fig. 5(a), we attributed the loss of coherence to our ability to distinguish paths from the final slit momentum whereas the same coherence loss in Fig. 5(d) would be attributed to an averaging over shifted patterns of unit visibility. The different visibilities in this random-average model are due entirely to averaging over patterns with varying amounts of shift relative to each other.

As mentioned before, if we do not measure the path-detector state, the total interference pattern can be calculated by randomly averaging over any basis for the detector such as its position or momentum. On the other hand, in this case if we do tag those atoms which leave the first screen in a particular position, we can recover a high-visibility interference pattern from within a featureless pattern.

V. THE FEYNMAN LIGHT MICROSCOPE

Consider the configuration shown in Fig. 6 in which atoms travel along the z direction, pass through a fixed double slit, and are collected on a screen at distance L away. A light field traveling along the x direction is used to indicate the path by scattering off the atom. For simplicity, we only consider elastic scattering and use the $\mathcal{S}$-matrix approach for this problem. Following Cohen-Tannoudji, Bardou, and Aspect [8], we denote by $\mathcal{S}(\mathbf{K}_i, \mathbf{K}_f; \mathbf{k})$ the amplitude of the elementary process in which a photon of initial momentum $\hbar\mathbf{K}_i$ scatters off an atom of momentum $\hbar\mathbf{k}$ to yield a final photon momentum of $\hbar\mathbf{K}_f$ and an atomic momentum of $\hbar(\mathbf{k}-\mathbf{K}_f+\mathbf{K}_i)$. If we neglect the Doppler effect, this amplitude is independent of the atomic momentum $\hbar\mathbf{k}$ and we may write

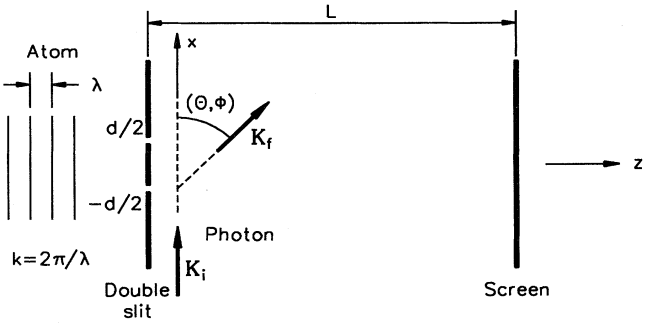

FIG. 6. The Feynman light microscope configuration. The path of particles (here taken to be atoms) through a screen with a double slit is observed by illuminating the slits with light. The state of the scattered light field is taken as the path detector.

$\mathcal{S}(\mathbf{K}_i, \mathbf{K}_f)$.

The magnitude $|\mathcal{S}(\mathbf{K}_i, \mathbf{K}_f)|$ depends on the projection of the polarization vector of the outgoing photon on the polarization vector of the incoming photon if the atomic dipole moment is aligned with the incoming polarization [9]. If we denote the polar and azimuthal angles of $\mathbf{K}_f$ relative to $\mathbf{K}_i$ by (θ, ϕ), the angular dependence of this amplitude is

$$|\mathcal{S}(\mathbf{K}_i, \mathbf{K}_f)| \propto \sqrt{1+\cos^2\theta}\,\delta(|\mathbf{K}_i| - |\mathbf{K}_f|) \tag{39}$$

for circular polarization, and

$$|\mathcal{S}(\mathbf{K}_i, \mathbf{K}_f)| \propto \sqrt{1+\sin^2\theta\cos^2\phi}\,\delta(|\mathbf{K}_i| - |\mathbf{K}_f|) \tag{40}$$

for linear polarization, where the delta function restricts our attention to elastic scattering. In order to assign the phase to the scattering amplitude, we consider scattering off an atom in a position eigenstate

$$|\mathbf{x}\rangle \propto \int d^3\mathbf{k}\,\exp(-i\mathbf{k}\cdot\mathbf{x})|\mathbf{k}\rangle. \tag{41}$$

For an initial joint state $|\mathbf{x}\rangle|\mathbf{K}_i\rangle$ of atom and photon, the outgoing state is proportional to

$$\int d^3\mathbf{K}_f\,\mathcal{S}(\mathbf{K}_i, \mathbf{K}_f)\exp[i(\mathbf{K}_i - \mathbf{K}_f)\cdot\mathbf{x}]\,|\mathbf{x}\rangle|\mathbf{K}_f\rangle. \tag{42}$$

Thus if we choose $\mathcal{S}(\mathbf{K}_i, \mathbf{K}_f)$ as purely real, this corresponds to the assumption that all the plane wave components of the scattered field are in phase at the location of the atom.

In this configuration, the state of the outgoing photon plays the role of the path detector. If the two slits are located at $x = \xi_1 = d/2$ and at $x = \xi_2 = -d/2$, the state $|D_\ell\rangle$ of the outgoing photon which couples with the path through the slit at ξ_ℓ is

$$|D_\ell\rangle \propto \exp(iK\xi_\ell)\int_0^{2\pi} d\phi \int_0^{\pi} d\theta\,\mathcal{S}(\mathbf{K}_i, \mathbf{K}_f) \times \exp(-iK\xi_\ell\cos\theta)K^2 \times \sin\theta|\mathbf{K}_f\rangle, \tag{43}$$

where $K = |\mathbf{K}_i| = |\mathbf{K}_f|$. The inner product of these two states (for either circular or linear polarization) is

$$\langle D_1|D_2\rangle = V(Kd)\exp(-iKd), \tag{44}$$

where

$$V(u) = \frac{3}{2}\left[\frac{\cos u}{u^2} + \frac{\sin u}{u} - \frac{\sin u}{u^3}\right]. \tag{45}$$

The modulus of this quantity $\mathcal{V} = |V(Kd)|$ gives the visibility of the interference pattern, in agreement with the result of Sleator *et al.* [10]. A graph of $V(u)$ is shown in Fig. 7. The total interference pattern is given by (11) which in this case is

$$P(x) \propto 1 + \mathrm{Re}[\exp(-iKd)V(Kd)\exp(ikdx/L)]. \tag{46}$$

For small Kd (i.e., light with wavelength large compared to d) such that $|V(Kd)| \approx 1$, the main effect of the illumination is to shift the central fringe of the interference pattern from $x = 0$ to $x = KL/k$. This is the expected momentum transfer from a single scattering event. For photons of smaller wavelength, the visibility is reduced.

We now consider the explanation for the loss of coherence in terms of the random-average model. First consider the possibility of localizing the position of the scattered photon immediately after its production. The pointer basis in this case is

$$|X\rangle = \int d^3\mathbf{K}\exp(-iK_xX)\,|\mathbf{K}\rangle, \tag{47}$$

where the integral is over all possible $\mathbf{K}$ and the subscript x indicates the x component of the vector. In order to calculate the partial interference patterns we find

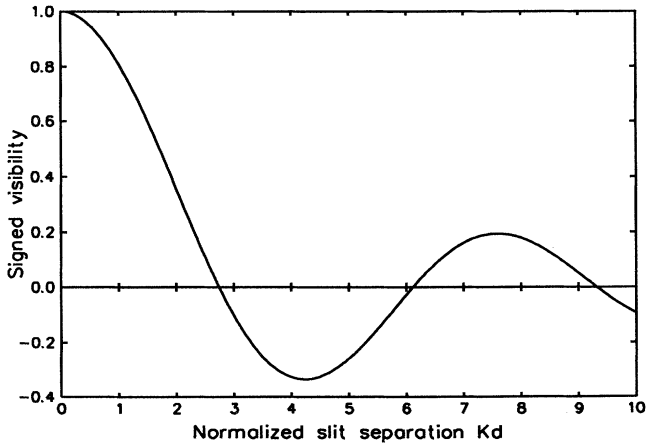

FIG. 7. The visibility of the atomic interference pattern as a function of Kd where K is the wave number of the light and d is the slit separation in the Feynman light microscope.

$$\langle X|D_\ell\rangle \propto \exp(iK\xi_\ell)\int_0^{2\pi} d\phi \int_0^{\pi} d\theta\, \mathcal{S}(\mathbf{K}_i,\mathbf{K}_f)\exp[iK(X-\xi_\ell)\cos\theta]K^2\sin\theta. \tag{48}$$

For circular polarization, this evaluates to

$$2\pi K^2\exp(iK\xi_\ell)\int_0^{\pi} d\theta \sin\theta\sqrt{1+\cos^2\theta} \times \exp[ik(X-\xi_\ell)\cos\theta] \tag{49}$$

and for linear polarization, this is

$$4K^2\exp(iK\xi_\ell)\int_0^{\pi} d\theta \sin\theta E(\sin^2\theta) \times \exp[ik(X-\xi_\ell)\cos\theta], \tag{50}$$

where $E(m)$ denotes the complete elliptic integral of the second kind. The integration over θ in each case can be performed numerically.

From these inner products, it is straightforward to calculate the partial interference patterns, the total interference pattern, the probability of localizing the photon at various possible positions, and the visibility of the conditional interference patterns. The only parameter affecting the visibility is the dimensionless combination Kd.

On the other hand, we may choose to measure the direction of travel of the scattered photon. Only the x component of the photon momentum is of interest and so for the purposes of displaying the joint probability distribution, we integrate in azimuth about the direction of the incident light beam.

If $\hbar\mathbf{K}_f$ is the momentum of the scattered photon,

$$\langle \mathbf{K}_f|D_\ell\rangle \propto \mathcal{S}(\mathbf{K}_i,\mathbf{K}_f)\exp[i(\mathbf{K}_i-\mathbf{K}_f)_x\xi_\ell]. \tag{51}$$

The partial interference pattern having measured a particular $\mathbf{K}_f$ is

$$P(\mathbf{K}_f,x)\propto \mathcal{S}(\mathbf{K}_i,\mathbf{K}_f)\big(1+\mathrm{Re}\,[\exp\{-i(\mathbf{K}_i-\mathbf{K}_f)_x d\} \times \exp(ikdx/L)]\big), \tag{52}$$

where the subscript x denotes the x component of the vector. Integrating over the azimuthal angle and changing the variable to K_{fx}, the x component of the momentum of the scattered photon, we find that

$$P(K_{fx},x)\propto (K_i^2+K_{fx}^2)\big(1+\mathrm{Re}\,\{\exp[-i(K_i-K_{fx})d] \times \exp(ikdx/L)\}\big), \tag{53}$$

where this result holds for either linearly or circularly polarized light. These patterns each have unit visibility and the central maximum is shifted to $x=(K_i-K_{fx})L/k$. This has a natural physical interpretation in terms of a momentum kick in the x direction imparted to the atom by the scattering of the photon. The total interference pattern is found by integrating over the possible values of K_{fx} from $-K_i$ to K_i and it is readily verified that the result is (46).

From Fig. 7, we see that if we choose $Kd=1$, the visibility is quite high ($\mathcal{V}\approx 0.81$). Figures 8(a) and 8(d) show how this result is obtained by the random-average model where we use the possible positions and x component of momentum of the scattered photon respectively as a description of the path detector. Since the photon wavelength is large, measuring the position of origin of the scattered photon does not well localize the atom. In Fig. 8(a), the range of probable photon positions forms a single peak over which the conditional visibility of the interference pattern is high. In Fig. 8(d), the physical explanation for the high visibility is that the momentum transfer from the photon to the atom is sufficiently small that the interference pattern is not washed out.

Figures 8(b) and 8(e) are for the opposite situation where $Kd\approx 9.3$ and the visibility is close to zero. If we consider measuring the position at which the scattered photon is emitted, we see that there are two distinct peaks, each corresponding to the atom going through one slit. The slits are sufficiently well separated that the paths are resolved by the measurement and interference is destroyed. The conditional visibility associated with each peak is low and so we have an average of single-slit patterns. On the other hand, from Fig. 8(e), conditional on measuring a particular momentum of the photon, the interference pattern has unit visibility. These perfect interference patterns are shifted by the momentum kick associated with the interaction with the photon. When the average is taken, the kicks are so large that the interference is lost.

Figures 8(c) and 8(f) are for $Kd\approx 4.2$ at which there is a local maximum in the visibility ($\mathcal{V}\approx 0.34$). Although the position distribution of the photon shown in Fig. 8(c) consists of two fairly well-separated peaks, a secondary maximum of one peak coincides with the maximum of the other so that the path is in fact not well determined. This can be also seen in the relatively high conditional visibilities associated with the probable photon positions. From these considerations it is clear that the oscillations in the visibility seen in Fig. 7 arise from the oscillations in the inner products $\langle X|D_\ell\rangle$ which describe how well a measurement of the photon position determines the atomic position.

The measurement of the photon position or momentum can be carried out (at least in principle) by including a lens which collects the scattered light and letting this light fall on a screen. If the distance of the lens from the slits and screen is arranged to be equal to twice the focal length of the lens, this gives an imaging configuration in which positions at which the light was scattered at the slits are mapped to positions on the screen. On the other hand if the distance of the lens from the slits and screen is equal to the focal length of the lens, various directions of photon emission are mapped to positions on the screen. Various additional complications arise due to the finite aperture size of a real lens, but a lens does provide a way of selecting a pointer basis for measuring the state of the outgoing photon.

From the above, the analogies between this configura-

tion and the Einstein recoiling slit should be clear. A measurement of the recoiling slit momentum is analogous to measuring the position of emission the scattered photon since each measurement localizes the atomic position to some extent. Under favorable conditions, the localization causes the visibility of the conditional interference patterns to fall and the loss of coherence is seen as an average of single-slit patterns. On the other hand, a measurement of the position of the recoiling slit is analogous to a measurement of the momentum of the scattered photon since in each case the conditional interference patterns have unit visibility but are simply shifted. Such a shift is indistinguishable from a momentum kick. The visibility of the final interference pattern depends on how these perfect interference patterns line up when they are averaged together.

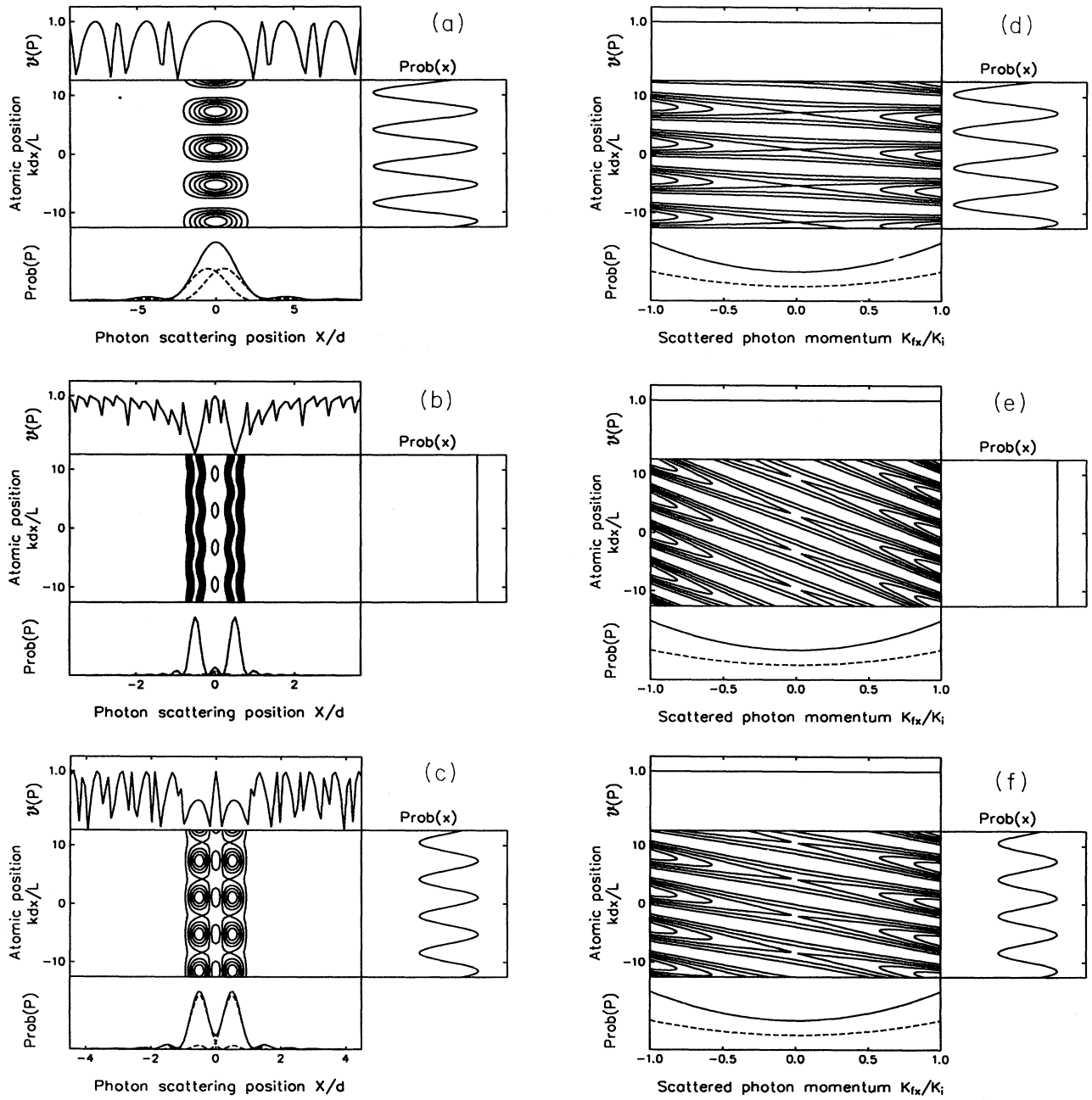

FIG. 8. Random-average model plots for the Feynman light microscope. Plots (a), (b), and (c) are for a measurement of the position from which the scattered photon is emitted while (d), (e), and (f) are for a meaurement of the x component of the scattered photon is measured. In plots (a) and (d) the product of the wave number of the light and the slit separation $Kd = 1$ and the resulting visibility is about 0.81. In plots (b) and (e), $Kd = 9.3$ and the resulting visibility is nearly zero. In plots (c) and (f), $Kd = 4.2$ and the resulting visibility is about 0.34. Refer to Fig. 3 for the key to the various plots.

VI. DOUBLE-SLIT EXPERIMENT WITH MICROMASER CAVITIES

We now analyze a configuration similar to that of Scully, Englert, and Walther [5] in which two independent cavities are placed immediately to the left of the slits as which-path detectors for excited atoms entering the system (Fig. 1).

Let $g_1(x)$ and $g_2(x)$ denote the couplings between the atom and the cavity fields which are proportional to the amplitudes of the mode functions of the two cavities. We assume that these mode functions each vanish where the other is nonzero and that at the positions of the slits $g_1(x_1) = g_2(x_2)$. Typically g_1 and g_2 might be sinusoidal functions representing two standing waves, but their exact forms away from the slit locations are unimportant. If we now quantize the modes as well as the atomic state, the interaction Hamiltonian may be written

$$H_I = \hbar g_1(x)(a_1\sigma_+ + a_1^\dagger\sigma_-) + \hbar g_2(x)(a_2\sigma_+ + a_2^\dagger\sigma_-), \tag{54}$$

where we have assumed the cavity fields are exactly resonant with the atomic transitions, a_i is the annihilation operator for the mode in cavity i and $\sigma_\pm$ are the usual pseudospin operators for the two-level atom.

If we write the state of the atom and the cavities as

$$|\psi\rangle = \sum_m \sum_n \int dx\, a_{mn}(x)\,|m,n;e,x\rangle + b_{mn}(x)\,|m,n;g,x\rangle\,, \tag{55}$$

where m and n denote the number of photons in cavities 1 and 2, respectively, and e and g refer to the state of the atom, we find that the amplitudes satisfy the coupled system of equations

$$i\,\dot{a}_{mn} = g_1(x)\sqrt{m+1}\,b_{m+1,n} + g_2(x)\sqrt{n+1}\,b_{m,n+1}, \tag{56}$$

$$i\,\dot{b}_{mn} = g_1(x)\sqrt{m}\,a_{m-1,n} + g_2(x)\sqrt{n}\,a_{m,n-1}. \tag{57}$$

If we denote the support of g_i (the set over which the function is nonzero) by S_i, we can write the solution of these equations as

$$a_{mn}(x,t) = \begin{cases} a_{mn}(x,0)\cos[g_1(x)\sqrt{m+1}\,t] - i\,b_{m+1,n}(x,0)\sin[g_1(x)\sqrt{m+1}\,t] & \text{if } x \in S_1 \\ a_{mn}(x,0)\cos[g_2(x)\sqrt{n+1}\,t] - i\,b_{m,n+1}(x,0)\sin[g_2(x)\sqrt{n+1}\,t] & \text{if } x \in S_2 \\ a_{mn}(x,0) & \text{otherwise,} \end{cases} \tag{58}$$

$$b_{mn}(x,t) = \begin{cases} -i\,a_{m-1,n}(x,0)\sin[g_1(x)\sqrt{m}\,t] + b_{mn}(x,0)\cos[g_1(x)\sqrt{m}\,t] & \text{if } x \in S_1 \\ -i\,a_{m,n-1}(x,0)\sin[g_2(x)\sqrt{n}\,t] + b_{mn}(x,0)\cos[g_2(x)\sqrt{n}\,t] & \text{if } x \in S_2 \\ b_{mn}(x,0) & \text{otherwise.} \end{cases} \tag{59}$$

Suppose that at $t = 0$ the atom enters in the excited state and that the cavities are in a superposition of Fock states

$$|D_0\rangle = \sum_m \sum_n c_{mn}|m,n;e\rangle, \tag{60}$$

so that $a_{mn}(x,0) = c_{mn}a(x)$ and $b_{mn}(x,0) = 0$. After interaction time t_i and passage through the slits, the joint state of atom and cavities is

$$\begin{aligned}|\psi\rangle \propto \sum_m \sum_n & c_{mn}a(x_1)\cos[g_1(x_1)\sqrt{m+1}\,t_i]\,|m,n;e,x_1\rangle \\ & + c_{mn}a(x_2)\cos[g_2(x_2)\sqrt{n+1}\,t_i]\,|m,n;e,x_2\rangle \\ & - i\,c_{m-1,n}a(x_1)\sin[g_1(x_1)\sqrt{m}\,t_i]\,|m,n;g,x_1\rangle \\ & - i\,c_{m,n-1}a(x_2)\sin[g_2(x_2)\sqrt{n}\,t_i]\,|m,n;g,x_2\rangle\,.\end{aligned} \tag{61}$$

In the following, we shall further assume that $a(x_1) = a(x_2)$ so that the distance between the source and each slit is the same and that the mode functions in the cavities are such that $g_1(x_1) = g_2(x_2) = g$.

The "detector" in this case consists of the state of the cavities and the final internal state of the atom. The states which couple to the two possible paths are

$$\begin{aligned}|D_1\rangle = & \sum_m \sum_n c_{mn}\cos[g\sqrt{m+1}t_i]|m,n;e\rangle \\ & -ic_{m-1,n}\sin[g\sqrt{m}t_i]|m,n;g\rangle,\end{aligned} \tag{62}$$

$$\begin{aligned}|D_2\rangle = & \sum_m \sum_n c_{mn}\cos[g\sqrt{n+1}t_i]|m,n;e\rangle \\ & -ic_{m,n-1}\sin[g\sqrt{n}t_i]|m,n;g\rangle,\end{aligned} \tag{63}$$

The inner product of the states is

$$\begin{aligned}\langle D_1|D_2\rangle = \sum_m \sum_n \{ & |c_{mn}|^2\cos[g\sqrt{m+1}t_i]\cos[g\sqrt{n+1}t_i] \\ & + c^*_{m-1,n}c_{m,n-1}\sin[g\sqrt{m}t_i] \\ & \times \sin[g\sqrt{n}t_i]\},\end{aligned} \tag{64}$$

where $\sum_m \sum_n |c_{mn}|^2 = 1$. This gives the visibility of the interference pattern.

A. Cavities initially empty

This is the situation considered by Scully, Englert, and Walther as a means of producing a which-path detector for the atom. If the cavities are initially empty, $c_{00} = 1$ and all other coefficients are zero. By choosing the

interaction time so that $gt_i = \pi/2$, we can ensure that the initially excited atom will deexcite during its passage through the cavities. The state after passage through the cavities and slits is simply

$$|\psi\rangle \propto |1,0;g,x_1\rangle + |0,1;g,x_2\rangle\,. \tag{65}$$

The detector states coupling to the two possible atomic paths are $|D_1\rangle = |1,0;g\rangle$ and $|D_2\rangle = |0,1;g\rangle$ which are orthogonal. From our general analysis, it is clear that there is zero visibility in the far-field interference pattern.

The random-average model requires that we calculate a joint probability distribution of the detector state and the far-field atomic interference pattern. Unlike the previous examples in which there is a natural continuum of states (position or momentum) in which the detector may be found, we need only consider a two-dimensional pointer basis for the cavities in this case. If we adopt the natural number state basis

$$|B_1\rangle = |1,0;g\rangle \quad \text{and} \quad |B_2\rangle = |0,1;g\rangle \tag{66}$$

it is clear that if the detector is measured in state $|B_\ell\rangle$, the atom is localized to slit ℓ and the partial interference pattern is a featureless single-slit pattern. The sum over these two single-slit patterns gives an overall pattern with zero visibility.

On the other hand we may choose to adopt an alternative description of the cavities using the states

$$|B_S\rangle = (|1,0;g\rangle + |0,1;g\rangle)/\sqrt{2}, \tag{67}$$

$$|B_A\rangle = (|1,0;g\rangle - |0,1;g\rangle)/\sqrt{2}. \tag{68}$$

These are also orthogonal and span the same space as the original states. Using this description, Eq. (65) may be written

$$|\psi\rangle = \frac{1}{\sqrt{2}}\,|B_S\rangle\,(|g,x_1\rangle + |g,x_2\rangle) + \frac{1}{\sqrt{2}}\,|B_A\rangle\,(|g,x_1\rangle - |g,x_2\rangle). \tag{69}$$

If we measure the cavities to be in state $|B_S\rangle$, the partial atomic state is $(|g,x_1\rangle + |g,x_2\rangle)/\sqrt{2}$. This atomic state produces a partial interference pattern of unit visibility with a central "bright" fringe of high probability. On the other hand, if we measure the cavities to be in state $|B_A\rangle$, the partial atomic state is $(|g,x_1\rangle - |g,x_2\rangle)/\sqrt{2}$. This atomic state produces a partial interference pattern of unit visibility but with a central "dark" fringe of low probability. The sum of the two partial interference patterns once again is featureless, but we have quite a different physical model for the coherence loss.

The intriguing possibility of implementing a "quantum eraser" is raised in the article by Scully, Englert, and Walther. In essence, this is a device which can detect whether the cavities are left in state $|S\rangle$ or in state $|A\rangle$ after the interaction. If on successive repetitions of the experiment (with the cavities reinitialized to the vacuum state between repetitions) each atom passing through the system is tagged as to whether it left the cavities in state $|S\rangle$ or in state $|A\rangle$, we see that each subclass of atoms will produce a far-field interference pattern of unit visibility but with the minima and maxima interchanged. When all the atoms are considered together however, no interference is observed. Insofar as a determination of whether the cavities are in state $|S\rangle$ or $|A\rangle$ prevents us from telling which path was taken by the atom, the recovery of the conditional interference patterns from the system is interpreted as a consequence of the "erasure" of the which-path information. This erasure may be performed at any time after the interaction and in particular after the atom has been detected. From our analysis it can now be seen that a quantum eraser can in principle also be implemented for the Einstein recoiling slit experiment or the Feynman light microscope. By simply tagging atoms associated with a particular final position of the recoiling slit or with a particular final momentum of the scattered photon, we recover conditional interference patterns of high visibility from the midst of total patterns with low visibility.

B. Cavities initially containing coherent radiation

By preparing the cavities initially in a vacuum state, we see that the atoms which leave the slits do not produce any interference fringes. We shall now show that if the cavities are initialized to coherent states of nonzero amplitude, interference is once again possible. In one sense this is not surprising since it may be thought that if we have a large mean number of photons in the cavities, the addition of a single extra photon from the atom will not be detectable and so no which-path information is available. However, we shall see that the visibility depends on the length of the interaction time in the field and that for longer interaction times, the visibility does decrease to zero.

If the cavities are initialized to coherent fields with amplitude α, the coefficients c_{mn} are given by

$$c_{mn} = \exp(-|\alpha|^2)\frac{\alpha^{m+n}}{\sqrt{m!n!}}. \tag{70}$$

We can plot the visibility of the resulting interference pattern by using Eq. (64). Figure 9(a) shows the result as a function of the normalized interaction time gt_i for low amplitude coherent fields with $\alpha = 0.1$. We see that the visibility oscillates at the Rabi frequency and it is easy to check that these oscillations are in phase with the probability that the atom is in the excited state when it leaves the cavities. This is not unexpected since the cavities are very close to vacuum states and so which-path information is readily available provided that the atom deexcites and leaves a photon in one of the cavities. If the atom leaves in the excited state, no path information is recorded and the visibility remains high.

Figure 9(b) is the corresponding graph for initial coherent amplitudes $\alpha = 4$ ($\overline{n} = 16$) in the two cavities. In Fig. 10, we display the probability that the atom leaves in the ground state after the interaction. Once again there are Rabi oscillations but these die away due to interference between the different oscillation rates for the dif-

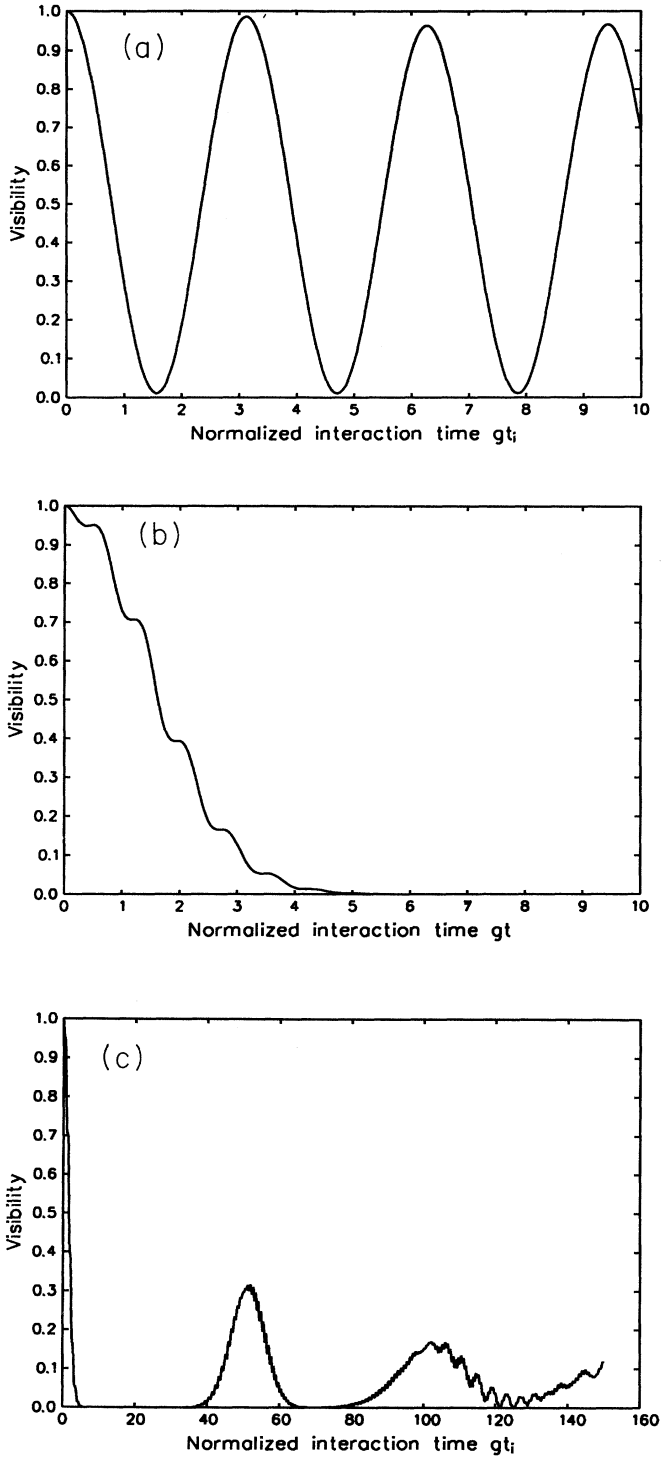

FIG. 9. Visibility as a function of the normalized interaction time gt_i for the two-slit experiment with micromaser cavities when the initial fields in the cavities are coherent. In (a), the field amplitudes are small $\alpha = 0.1$, whereas in (b) and (c) the initial field amplitudes are large, $\alpha = 4$. Graph (c) is plotted with a different horizontal axis from (b) to show the collapses and revivals in the visibility at long interaction times.

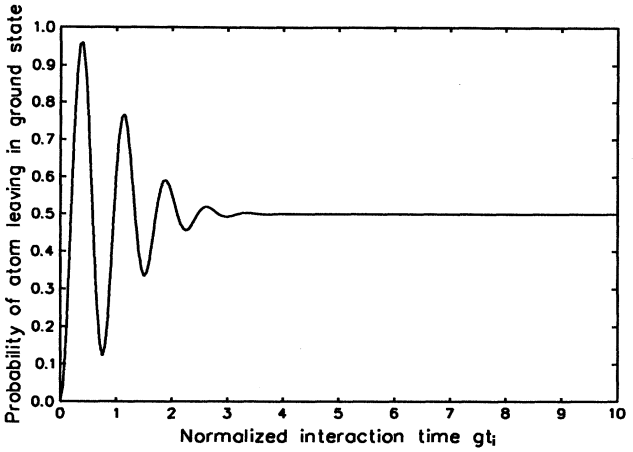

FIG. 10. The probability that an atom exits from the cavities in the ground state as a function of the normalized interaction time gt_i for the two-slit experiment with micromaser cavities for the situation described in Fig. 9(b) showing the decay of Rabi oscillations.

ferent number states which make up the coherent state. We notice that after the first half-cycle of the Rabi oscillation when the atom has a high probability of deexciting within a cavity and leaving in the ground state, the visibility of the interference pattern is still high. Thus, unlike the previous situation, it is not possible to determine which-path information from the cavities. After several Rabi cycles however, the visibility falls to zero. The interaction of the atom with the coherent field still causes a destruction of the interference but this process is more gradual than when the cavities are initially empty. Note that for large interaction times we do have a loss of coherence even though the path of the atom through the cavity cannot be determined by simply counting the photons in the cavities. This simply emphasizes the result discussed earlier in connection with the recoiling slit that not having path information is a necessary but insufficient condition for an interference pattern of high visibility.

The damping of the Rabi oscillations due to the superposition of different oscillation rates produced by a superposition of many photon number states in the cavities leads to the possibility of subsequent collapses and revivals in the oscillations as these rates beat with each other. A consequence of this is that the visibility predicted by Eq. (64) also shows these collapses and revivals [11] as shown in Fig. 9(c) for longer interaction times.

VII. DISCUSSION

In this paper, we have analyzed the double-slit experiment which is perhaps the simplest of all situations in which the interference of probability amplitudes occurs. When such a system is coupled to an environment, a loss of coherence can occur, the extent of the loss being determined completely by the initial state of the environment and the nature of the interaction. If however we seek

a physical mechanism for this loss, this is not uniquely determined but rather depends on the way in which we choose to describe the environment. Conditional upon measuring the environment to be in a particular state, the effective complex amplitudes at the slits are altered. If this is simply a change in phase, the effects can be interpreted as and are indistinguishable from a momentum kick. However if the change alters the moduli of the slit amplitudes, we say that a (possibly imprecise) localization of the atom to one path or other has occurred.

The random-average model shows that loss of coherence may always be described in terms of a stochastic disturbance to the system due to the coupling with an environment. This disturbance is random insofar as it is not possible to determine *a priori* the result of measuring the environment after the interaction has occurred. However, this randomness does not prevent sufficiently careful measurements of the environment from giving us information which reveals the exact nature of the disturbance. Collecting such information is the basis of "quantum erasers" which may be implemented for all the systems discussed.

The relationship between the orthogonality of the final environment states and the random dephasing of the system wave function discussed by Stern, Aharonov, and Imry [1] is seen to be readily explicable in terms of the random-average model provided that the concept of "dephasing" is extended to cover the full range of possible changes to the system wave function when the entangled state of system and environment is projected out along a pointer basis of the environment. The effect of a probabilistic average over any pointer basis for the environment reduces the degree of coherence by precisely the amount predicted by taking the inner product of final environment states.

ACKNOWLEDGMENTS

We thank M. Collett and M. Scully for helpful discussions. This work was supported by the University of Auckland Research Committee.

[1] A. Stern, Y. Aharonov, and Y. Imry, Phys. Rev. A **41**, 3436 (1990).
[2] M. Jammer, *The Philosophy of Quantum Mechanics* (Wiley, New York, 1974), p. 121.
[3] F. Belinfante, *Measurement and Time Reversal in Objective Quantum Theory* (Pergamon, New York, 1975), p. 32.
[4] R. Feynman, R. Leighton, and M. Sands, *The Feynman Lectures on Physics* (Addison-Wesley, Reading, MA, 1965), Vol. 3.
[5] M. Scully, B-G. Englert, and H. Walther, Nature **351**, 111 (1991).
[6] B-G. Englert, J. Schwinger, and M. Scully, *New Foundations in Quantum Electrodynamics and Quantum Optics*, edited by A. Barut (Plenum, New York, 1990), p. 513.
[7] W. Wooters and W. Zurek, Phys. Rev. D **19**, 473 (1979).
[8] C. Cohen-Tannoudji, F. Bardou, and A. Aspect, *Tenth International Conference on Laser Spectroscopy*, edited by M. Ducloy, E. Giacobino, and G. Camy (World Scientific, Singapore, 1992), p. 3.
[9] R. Loudon, *The Quantum Theory of Light*, 2nd ed. (Oxford University Press, Oxford, 1983), Chap. 8
[10] T. Sleator, O. Carnal, T. Pfau, A. Faulstich, H. Takuma, and J. Mlynek, *Tenth International Conference on Laser Spectroscopy*, edited by M. Ducloy, E. Giacobino, and G. Camy (World Scientific, Singapore, 1992), p. 264.
[11] J.H. Eberley, N.B. Narozhny, and J.J. Sanchez-Mondragon, Phys. Rev. Lett. **44**, 1323 (1980).